App. Envi. Res. 40(1) (2018): 75-86

Applied Environmental Research

Journal homepage: http://www.tci-thaijo.org/index.php/aer

Morphometric Temporal Change Analysis for the River Nile Forced Bends using RS/GIS Techniques: Case Study of Damietta Branch of the Nile River, Egypt

Reham A.B. Aborahma[1,*], Wael E. Mahmod[1,2], Hassan E.B. Fath[1]

[1] Irrigation and Hydraulics Engineering Department, Faculty of Engineering, Egypt-Japan University of Science and Technology, Alexandria, Egypt
[2] Civil Engineering Department, Faculty of Engineering, Assiut University, Assiut, Egypt
[*] Corresponding author: Email: Reham.Abo-Rahma@ejust.edu.eg, Reham_aborahma@f-eng.tanta.edu.eg

Article History
Submitted: 3 August 2017/ Accepted: 15 December 2017/ Published online: 28 February 2018

Part of this manuscript was presented in the 4th EnvironmentAsia International Conference on Practical Global Policy and Environmental Dynamics, June 21-23, 2017, Bangkok, Thailand

Abstract

The River Nile is one of the world's longest rivers. The Damietta branch in Egypt is important as a major source of irrigation and navigation path from Cairo to the Mediterranean Sea. Morphological changes in this branch of the Nile occurred following construction of the Aswan High Dam, which affected sedimentation and erosive flow, especially at bends in the river. In this study, morphometric temporal changes were investigated for the forced bends using Remote Sensing (RS) and Geographical Information System (GIS) techniques for a study period between 1987 and 2015. In addition, a comparative study was performed among three image classification techniques; onscreen digitizing, maximum likelihood classification and histogram thresholding techniques. A field map of the river banks for the year 2000 was used to verify morphometric behavior of the forced bends extracted from the satellite images. The study showed that the maximum likelihood classification technique showed good performance in shoreline detection, with percentage error of only 0.42 % compared with observed data. Results show significant morphometric changes of the bank status for the forced bends studied. The forced bend named Sherpas was found to have the highest average annual rate of erosion, with a value of 1.62 m a^{-1}. The maximum average annual rate of sedimentation was located at the inner bank of Sawalem forced bend, with a value of 1.0 m a^{-1}. The maximum erosion and sedimentation rates achieved the greatest values within the period 1987 to 1998.

Keywords: Morphometric changes; Forced bends; Remote sensing; Geographical information system; Damietta branch

Introduction

The flow of fluids through channels, especially in bends, causes secondary currents which in turn is one of the most important causes of erosion along the outer curve of the bends and sedimentation at the inner curve. This phenomenon is evident and escalated in the case of severe sharp curves which are named "forced bends". The Damietta branch of the Nile features a total of ten forced bends from its origin at the downstream delta barrage (south of Cairo governorate) to the Mediterranean Sea in the north.

The river channel changes from its straight phase to meandering, and finally braiding. Up until the late 1970s, it was thought that the secondary flow at the bend consisted of a single skew-induced cell. However, close to the eroding outer bank, there is often a smaller cell of reverse rotation. The skew-induced secondary cell does not extend to the inner bank either. Flow over the upper point-bar is directed radially outward throughout the whole water column because the outwards acting centrifugal force on the curved flow overcomes the inward pressure gradient force. The secondary circulation pattern at a river bend cross section shows that the main circulation cell is limited to the deepest part of the section; it has been suggested that this outward flow has a significant effect on the point-bar growth as shown in Figure 1 [1-2]. The primary longitudinal currents are disturbed by the secondary ones, causing more deposition by the decreasing phase shift angle which leads to braiding [3]. On a smaller scale, the process of bending in channels results from the process of sediment transfer [4-5]. On the other hand, cross-stream circulation is imposed on the downstream motion- a characteristic phenomenon for the channel bends [6]. Also, a near balance in the centrifugal force and cross-stream pressure gradient are responsible for the cross-stream velocity field through the bend, which consist of the outward velocity near the surface and inward velocity near the bed across the entire channel width. In addition, development of a point bar in a curved channel greatly modifies the pattern of flow and the downstream and cross stream force balances [2].

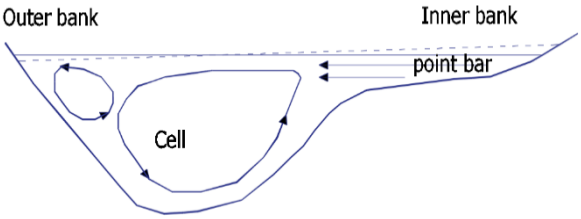

Figure 1 Balance between centrifugal force and pressure gradient.

The physical characteristics of bends were studied using hydrographic survey maps such as wave length, radius of curvature, and stream length [7]. On the other hand, another study illustrated that the outer curve of Damietta branch will suffer from erosion with an expected erosion volume of 12,921.90 m^3 [8]. Landsat imagery and field observations were used to study the meandering and bank erosion of the River Nile and its environmental impact on the area between Sohag and El-Minia, Egypt and an onscreen digitizing method was used to obtain the shoreline of the study reach [9]. The histogram thresholding technique showed an accurate result for separating the waterbody from non-waterbody compared with ground truth observations, by using Band 5. Band 5 exhibits strong contrast between land and water features due to the high degree of absorption of mid-infrared energy by water (even turbid water) and the strong reflectance of mid-infrared by vegetation and natural features in this range [10]. On the other hand, the maximum likelihood classification was used to differentiate between several classes in one image [11]. River bank erosion is a complex phenomenon in which many factors affect the erosion process such as flow, sediment transport,

bank properties and water qualities. The bank properties induce the bank materials weight and texture, shear strength and cohesive strength, physicochemical properties, bank height and cross-sectional shape, ground water level and permeability, stratigraphy, tension cracks, as well as vegetation and constructions [12].

This study aims to investigate the morphometric temporal changes for Damietta branch forced bends. Three techniques for image classification (referred to above) were used to assess the Damietta branch shoreline for the study period (1987-2015) and their accuracy and utility evaluated and compared.

Study area

The geographical location for Damietta branch lies between latitude: 30° 10' 26" N, longitude: 031° 08' 22" E and latitude: 31° 31' 37" N, longitude: 031° 50' 41" E. Six forced bends of Damietta branch were studied in this research, as identified on the map in Figure 2.

Land use around the studied bends is varied including agriculture and urbanization. The agriculture represents dominant land use classes as shown in the composite Landsat image for the year 2015, as shown in Figure 3.

Materials and methods

1) Data set

Ten satellite images were used for Damietta branch, downloaded from the United States Geological Survey (USGS) server to cover Damietta branch between 1987 and 2015. Eight images were Landsat_5/TM acquired in 1987, 1998, 2000 and 2003. The remaining two images were Landsat_8/ETM acquired in 2015 as shown in Table 1 and Figure 3. These images were taken for the summer season, from May to August, to avoid seasonal effects. Winter in Egypt is characterized by clouds and rain, which complicate interpretation and lead to errors in image pre-processing [13]. In addition, to avoid the change in seasonal water levels; as in Egypt in the winter, from November to March, the chances of rainfall are increasing. Therefore, the Egyptian government, represented by the Ministry of Water Resources and Irrigation (MWRI), does not pump water to the water-ways depending on the rain water in irrigation. Therefore, in this period the water levels in the river are lower than the rest of the year.

A field map for the river banks for the year 2000 was used in the present study for verification process. This map was obtained from the Hydraulic Research Institute (HRI).

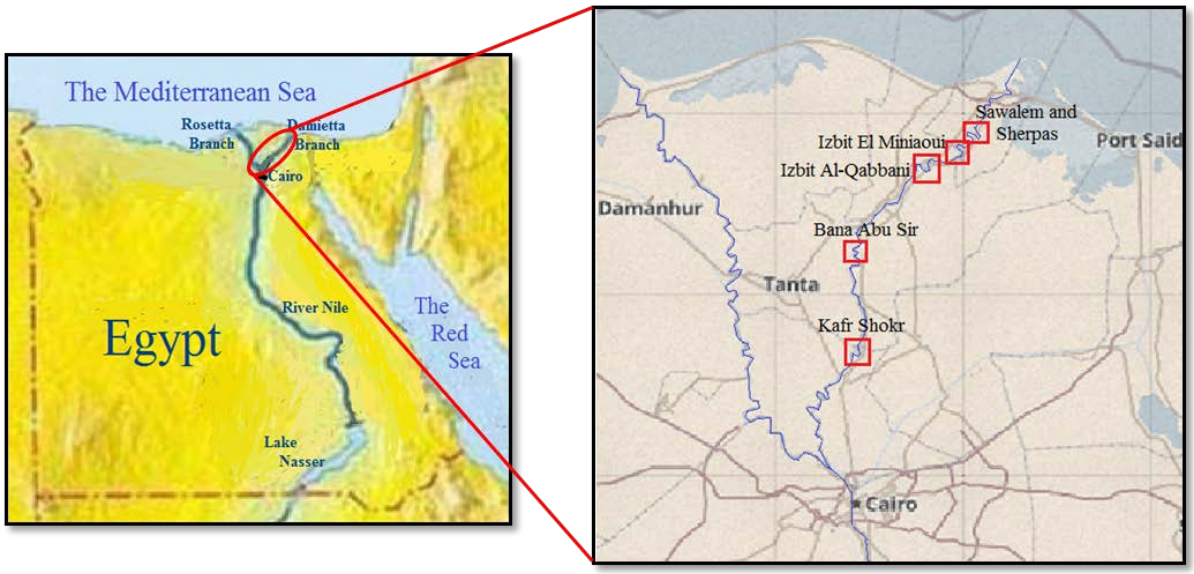

Figure 2 The geographical location for Damietta branch and the studied forced bends.

a) Kafr Shokr

b) Bana Abu Sir

c) Izbit Al-Qabbani

d) Izbit El Miniaoui

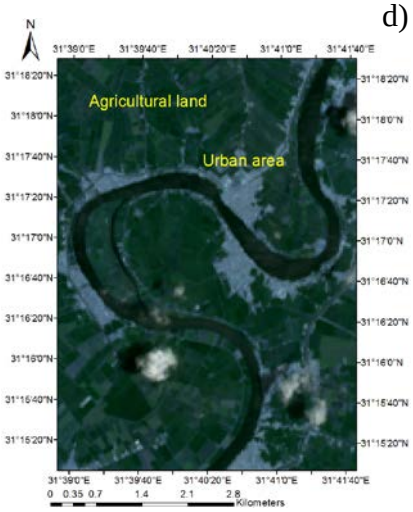

e) Sawalem and Sherpas

Figure 3 Landsat image for the studied forced bends along Damietta branch for 2015 (Landsat_8/ETM, Path/Row 176/39 and 176/38).

Table 1 Characteristics of the images used in this study

Acquired Date	SpaceraftID/ sensor	Path/row	Pixel size (m)	Coordinate system/datum	Zone
Jul 27, 1987	Landsat_5/TM	176/39	60	UTM/WG84	36 North
Jun 07, 1998	Landsat_5/TM	176/39	30	UTM/WG84	36 North
May 11, 2000	Landsat_5/TM	176/39	30	UTM/WG84	36 North
Jul 07, 2003	Landsat_5/TM	176/39	30	UTM/WG84	36 North
Jul 08, 2015	Landsat_8/ETM	176/39	30	UTM/WG84	36 North
Jul 27, 1987	Landsat_5/TM	176/38	60	UTM/WG84	36 North
Jun 07, 1998	Landsat_5/TM	176/38	30	UTM/WG84	36 North
May 11, 2000	Landsat_5/TM	176/38	30	UTM/WG84	36 North
Jul 07, 2003	Landsat_5/TM	176/38	30	UTM/WG84	36 North
Jul 08, 2015	Landsat_8/ETM	176/38	30	UTM/WG84	36 North

2) Image preprocessing

Erdas Imagine 9.1 are used for checking images against defects such as shadows and gaps. Also, all images were corrected radiometrically and geometrically. Then, a composite image for every image was obtained using the RGB bands. For Landsat_8/ETM, Band 2-blue, Band 3-green and Band 4-red. But for Landsat_5/TM, Band 1-blue, Band 2-green and Band 3-red.

ArcGIS 10.2 was used for analysis of data and visualization of results. In addition, field observations for Damietta branch were also made for verification purposes.

3) Image post-processing

Three remote sensing techniques were used to extract data from the satellite images, including onscreen digitizing, maximum likelihood classification and histogram thresholding technique method as shown in Figure 4. These methods were used to estimate the surface water area for the studied forced bends during the study period. Also, a field map for the river was used for verification purposes.

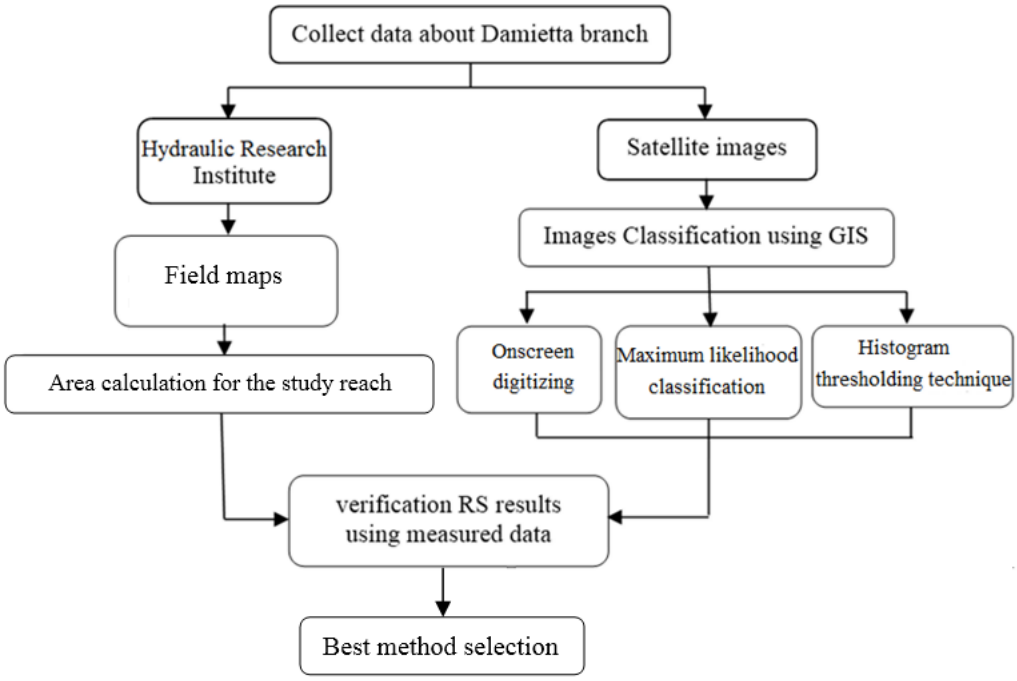

Figure 4 Flow chart for research methodology.

3.1) Onscreen digitizing

The shoreline for Damietta branch, Nile River was defined by drawing the borders onscreen on the image according to the vision in the differentiation between the waterbody and land [9]. For more accurate results, pixel digital number equal to 50 was selected to separate the borders of the river from the land.

3.2) Maximum likelihood classification

The classification process was used to separate the land-cover units in order to change the detection for each type [11]. Considering Bayes' theorem, the maximum likelihood classifier was obtained as illustrated in Eq. 1 [14].

$$dk(g) \geq dj(g) \quad \text{for all j=1,….K} \qquad \text{(Eq. 1)}$$

Where $dk(g)$ is a class-specific probability density function.

For suitable classification, a composite image conducted for all images was then used to enable classification. The maximum likelihood classification by support vector machine algorithm was made for the classification of the ten images into four land-cover classes, which are recognized as follows: Nile river, seawater, agricultural land and urban. The shore line of the Damietta branch was then obtained.

3.3) Histogram thresholding technique

The shoreline can be extracted from a single-band image, band 5, since the reflectance of water is nearly equal to zero in reflective infrared bands. This can be achieved, for example, by histogram threshold on one of the infrared bands of Thematic Mapper (TM) or Enhanced Thematic Mapper plus (ETM+) imagery [10].

4) Sinuosity calculation

The channel sinuosity of a reach, here called the sinuosity index (S.I.), is defined by the ratio of length of channel to length of meander-belt axis. The sinuosity index value for a channel can be divided into three categories: i) straight S.I. < 1.05 ii) sinuous 1.05 < S.I. < 1.5 and iii) meander S.I. > 1.5 [15].

Results and discussion

1) Comparative study

Observed field data were used to verify the results of the three remote sensing techniques (onscreen digitizing, maximum likelihood classification and histogram thresholding technique) to accurately locate the banks of the river in the forced bend locations. The surface water area for the length of each bend was calculated with the three techniques for the year 2000, then compared with the measured surface water area for the same year as shown in Figure 5.

The percentage error between the actual area for year 2000 and the calculated areas obtained from the three remote sensing techniques was calculated as shown in Table 2 using Eq. 2 as follows:

$$Error\% = \frac{\text{Actual area - calculated area}}{\text{Actual area}} \qquad \text{(Eq. 2)}$$

It is concluded that the onscreen digitizing method has the lowest error rate. Accordingly, on screen digitizing method was subsequently used to complete the morphometric temporal changes for the studied forced bends.

2) Morphometric changes for the studied forced bends

The morphometric analysis for the studied forced bend shows that the bend is subjected to erosion on the outer curve and sedimentation on the inner curve as shown in Figures 6 to 10. These changes are mainly due to secondary currents generated in the bends. Also, sedimentation and erosion processes are modified by the stone heads situated in the bending sites (Figure 3b, and 3c). These date back to before the establishment of the Aswan High Dam, which caused major morphological changes in these locations and have influence on deposition and erosion rates such in Bana

Abu Sir forced bend and Izbit Al-Qabbani forced bend as shown in Figure 7 and Figure 8, respectively. On the other hand, Izbit El Miniaoui forced bend and Sawalem forced bend have islands as shown in Figures 9 and 10, respectively. These islands were affected by secondary currents which led to changes in their shapes and areas. For the Sherpas forced bend, it is worth mentioning that the roads along the banks will be a risk because of deterioration of the river bank, which increases the risk of road collapse, as shown in Figure 10.

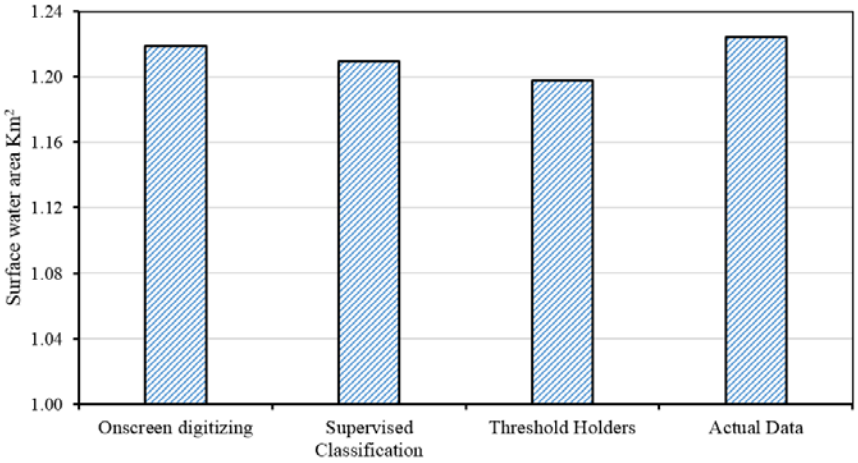

Figure 5 Surface water areas (km^2) for the year 2000.

Table 2 Percentage error for the three techniques

Method	Surface water area for year 2000	% Error
Actual area	1.224117	0
Onscreen digitizing	1.218961	0.4212
Maximum likelihood classification	1.209634	1.1831
Histogram thresholding method	1.197803	2.1497

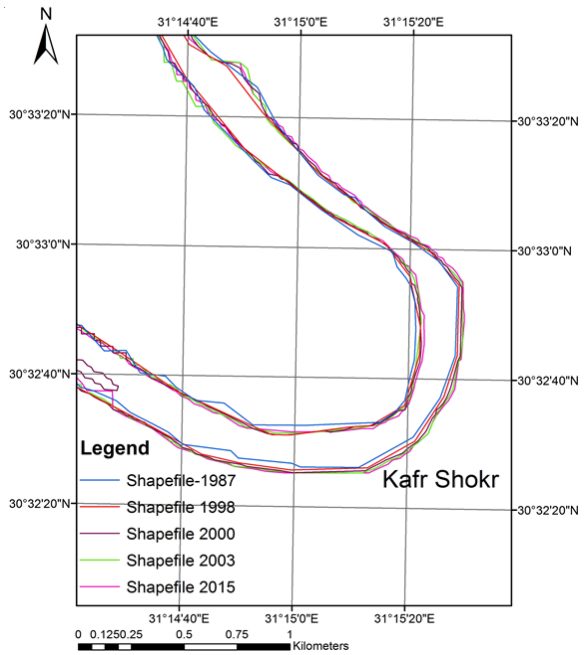

Figure 6 Temporal changes for Kafr Shokr forced bend.

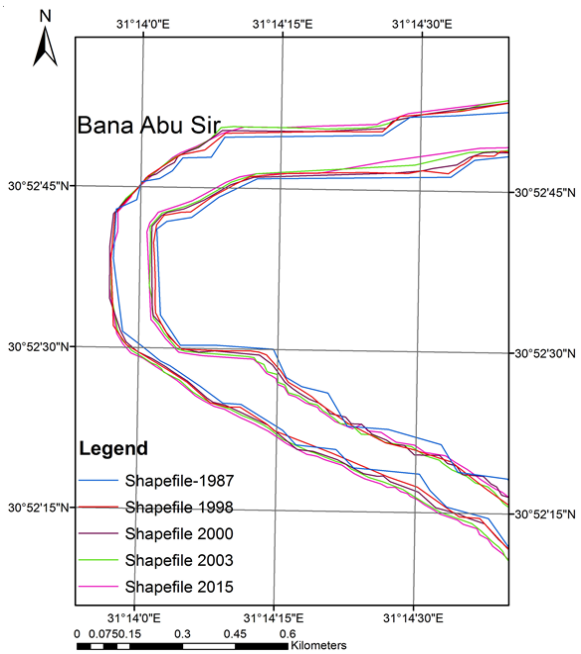

Figure 7 Temporal changes for Bana Abu Sir forced bend.

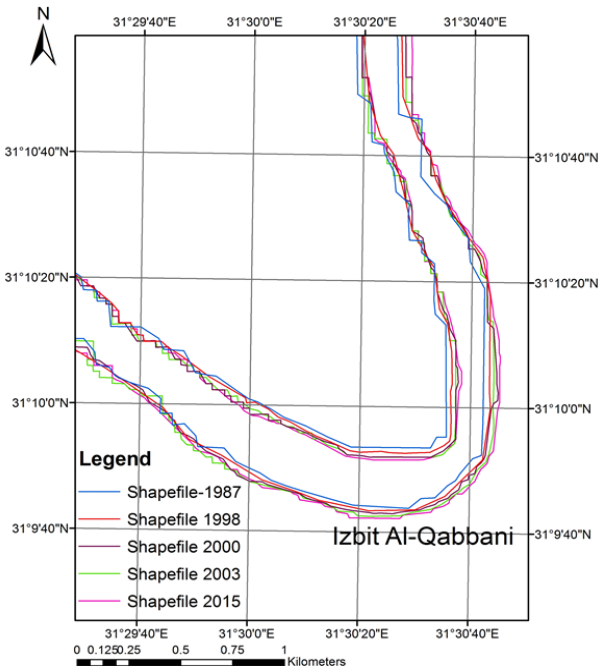

Figure 8 Temporal changes for Izbit Al-Qabbani forced bend.

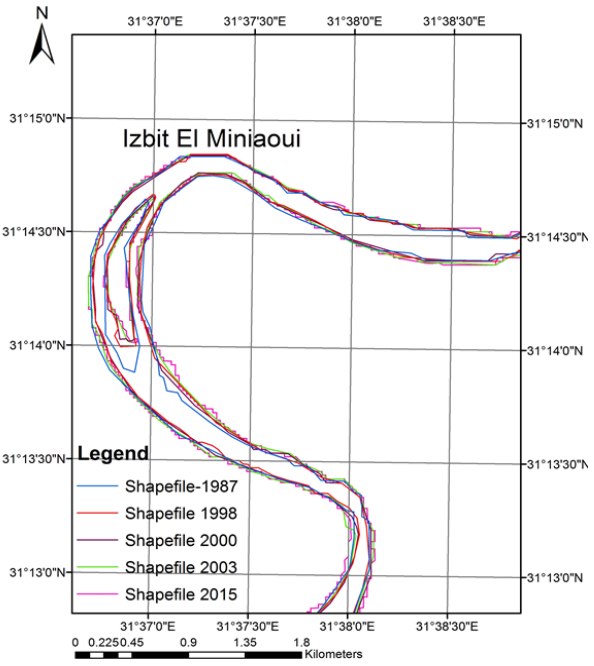

Figure 9 Temporal changes for Izbit El Miniaoui forced bend.

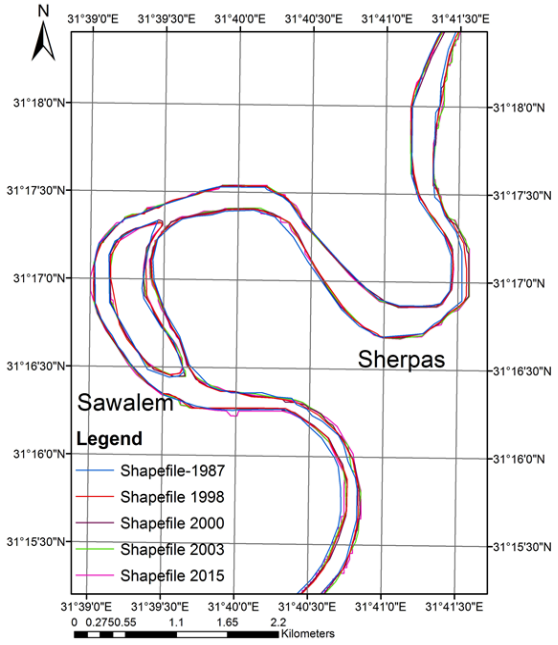

Figure 10 Temporal changes for Sawalem and Sherpas forced bend.

3) Meander parameters investigation

The meander parameters of the forced bends of Damietta branch were calculated as shown in Table 2 according to the meander parameters stated by Leopold et al. [5] and Sadek et al. [7]

The sinuosity index was calculated for the studied six bends of the Damietta branch, then compared with published values by Sadek et al. [7], who calculated the S.I., with the aid of field observation maps. Percentage errors for the two values of S.I. was obtained using Eq. 3 as shown in Table 3.

$$Error\% = \frac{\text{calculated S.I.} - \text{published S.I.[7]}}{\text{calculated S.I.}} \quad \text{(Eq. 3)}$$

It may be concluded from the comparison between the calculated S.I. and the previous one that the percentage error did not exceed 0.46 % as shown in Table 3. Also, all studied forced bends are classified as meanders according to [9], as the S.I. for all of them exceeds 1.5.

4) Forced bends characteristics

The surface water area of the studied forced bends was calculated as shown in Table 4 and Figure 11 for the study period between 1987 and 2015.

It is clear from Figure 11 that the surface water area changes over the years are mainly related to erosion and sedimentation rates. Also, one can say that the surface water area of the studied forced bends is increasing continuously. This means that the erosion rates were higher than the sedimentation rates in this study. The results show also that Bana Abu Sir forced bend has the maximum surface water area, increasing from 0.394 km^2 in 1987 to 0.456 km^2 in 2015. On the other hand, Kafr Shokr forced bend has the smallest surface water area, with a value of 0.12 km^2 in 1987 and 0.126 km^2 in 2015.

Table 3 Meander parameters of studied forced bends

Name	km	Bend length	Meander belt axis	Calculated S.I.	Published S.I. [7]	Error %
Kafr Shokr	95.00	7,302	2881.08	2.271935	2.44	-0.0740
Bana Abu Sir	139.50	3,621	3214.00	2.152794	1.88	0.1267
Izbit Al-Qabbani	194.50	7,535	1682.00	1.770026	1.91	-0.0791
Izbit El Miniaoui	214.50	7,734	4257.00	2.268700	2.05	0.0964
Sawalem	222.00	8,023	3409.00	3.645161	1.96	0.4623
Sherpas	227.50	6,128	2201.00	2.023110	2.60	-0.2852

Table 4 The surface water area of the studied forced bends

Name	Area (km^2)				
	1987	1998	2000	2003	2015
Kafr Shokr	0.120979	0.114352	0.121493	0.135930	0.126515
Bana Abu Sir	0.394019	0.420710	0.428355	0.453809	0.456154
Izbit Al-Qabbani	0.173159	0.175426	0.183011	0.178905	0.177257
Izbit El Miniaoui	0.175217	0.175537	0.17842	0.187521	0.195895
Sawalem	0.314154	0.299038	0.307682	0.317043	0.321841
Sherpas	0.125662	0.119615	0.123073	0.126817	0.128736

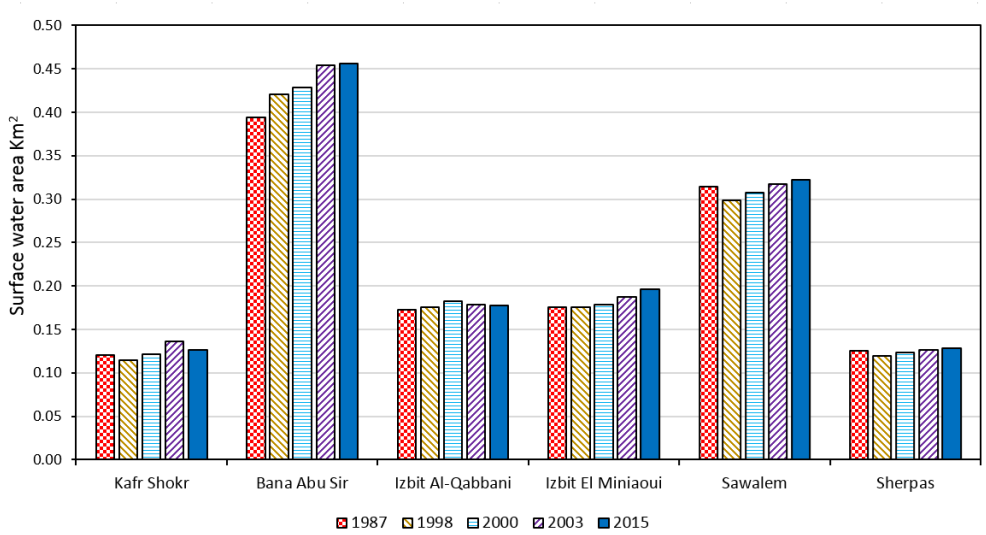

Figure 11 The surface water area of the studied forced bends in km^2.

The annual erosion rate (m) and annual sedimentation rate (m) were calculated during the study as shown in Table 5, Table 6, Figure 12 and Figure 13 for all bends. Also, the average annual erosion and average annual sedimentation rates (m a^{-1}) were obtained. The results show that the annual erosion rate in the first period, from 1987 to 2003, increased in most forced bends. However, from 2003 to 2015 this rate began to decrease due to the protection measures implemented by the MWRI and the Nile Research Institute (NRI). Figure 12 and Figure 13 show that Sherpas forced bend has the greatest average annual erosion rate with value of 1.62 m a^{-1}, while the minimum was for Bana Abu Sir with a rate of 0.56 m a^{-1}. The highest average annual sedimentation rate (1.0 m a^{-1}) was found at Sawalem forced bend, with the lowest at Sherpas (0.66 m a^{-1}).

Table 5 Annual erosion rates for the studied forced bends

Name	Annual erosion rate (m a^{-1})				Average annual erosion rate (m a^{-1})
	1987-1998	1998-2000	2000-2003	2003-2015	
Kafr Shokr	1.27	3	2	0.67	1.2765
Bana Abu Sir	0.9	0.5	0.67	0.167	0.56
Izbit Al-Qabbani	2.36	3.5	1	1.08	1.4753
Izbit El Miniaoui	0.54	2	2	0.75	1.0322
Sawalem	0.9	1	1	0.5	0.8522
Sherpas	2.09	3.5	2	1.25	1.6268

Table 6 Annual sedimentation rates for the studied forced bends

Name	Annual sedimentation rate (m a^{-1})				Average annual sedimentation rate (m a^{-1})
	1987-1998	1998-2000	2000-2003	2003-2015	
Kafr Shokr	1.09	2	2	0.67	0.6856
Bana Abu Sir	0.9	3.5	2.67	0.25	0.9356
Izbit Al-Qabbani	2	2.5	1	0.58	0.964
Izbit El Miniaoui	0.63	3	2.3	0.67	0.7
Sawalem	1	1.5	1.33	0.67	1
Sherpas	0.72	1.5	0.67	0.25	0.66

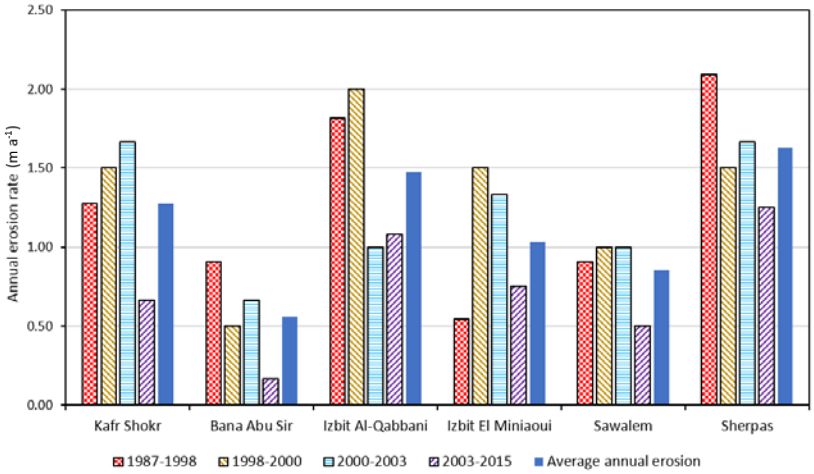

Figure 12 The Annual erosion rate (m a^{-1}).

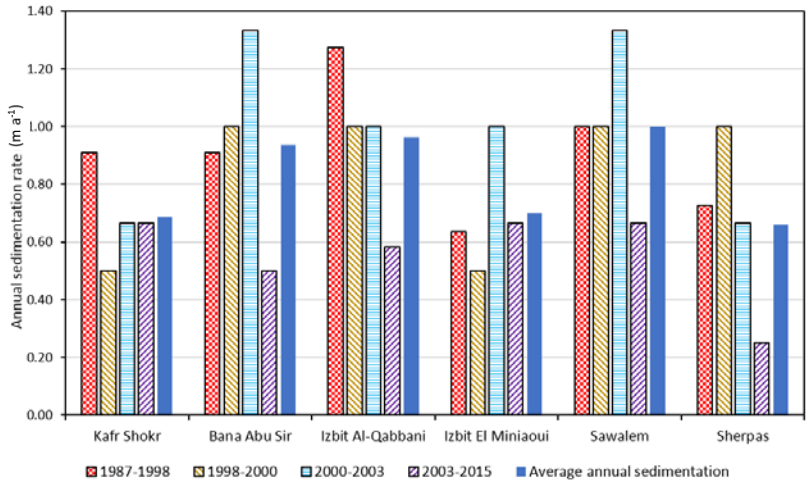

Figure 13 The Annual sedimentation rate (m a^{-1}).

Conclusion

Satellite images were used to record temporal changes in the forced bends along Damietta branch of the Nile River in Egypt, using GIS and RS techniques. Onscreen digitizing, maximum likelihood classification and histogram thresholding technique were used to delineate the banks of the river forced bends over the study period. Comparative analysis was performed for the image classification techniques and the field maps for the year 2000 which led to selection of the onscreen digitizing method for the morphometric analysis as the most accurate method. The surface water area of Bana Abu Sir forced bend shows the maximum surface area compared with the studied forced bends. The area temporal change of this bend was found to be 0.394 km^2 in 1987, increasing to 0.456 km^2 by 2015. Annual erosion and sedimentation rates were calculated for all forced bends. It was found that Sherpas forced bend exhibited the highest average annual erosion rate (1.62 m a^{-1}), while the highest average annual sedimentation rate was found at Sawalem forced bend (1.0 m a^{-1}). The secondary flow causes deposition along the concave curve and erosion along the convex curve, negatively affecting the stream course and surrounding areas along the river. This study sheds light on the need for action by the relevant authorities to implement urgent protection measures at the most vulnerable forced bends in order to avoid worsening adverse impacts resulting from morphometric changes at these sites.

Acknowledgments

The first author would like to thank the Egyptian Ministry of Higher Education (MoHE) for granting her the Ph.D. scholarship. Also, the authors are grateful to E-JUST and JICA for their generous support and for providing the tools needed for this research.

References

[1] Markham, A.J., Thorne, C.R., Geomorphology of gravel-bed river bends. Dynamics of Gravel-bed Rivers, 1992, 433-56.

[2] Smith, W., Dietrich, E., Dungan, J., Influence of the point bar on flow through curved channels, Water Resources Research, 19, 1983, 1173-92.

[3] Njenga, K.J., Kioko, K.J., Wanjiru, G.P. Secondary current and classification of river channels. Applied Mathematics, 2013, 4, 70-78.

[4] Fagherazzi, S., Emmanuel J.G., David J. F. The effect of bidirectional flow on tidal channel planforms. Earth Surface Processes and Landforms, 2004, 29, 295-309.

[5] Leopold, L., Wolman, M. Miller, J. Fluvial processes in geomorphology, San Francisco, CA: 1964, 79-80.

[6] Graf, W.H., Blanckaert, K. Flow around bends in rivers. In The 2nd International Conference New Trends in Water and Environmental Engineering for Safety and Life: Eco-compatible Solutions for Aquatic Environments. Capri (Italy), 2002.

[7] Sadek, N., Salama, R., Kamal, N. Effect of bank erosion and bend types on the effciency of Dammitta branch navigational path, Eighteenth International Water Technology Conference, IWTC18 Sharm ElSheikh, 12-14 March 2015, 70-86.

[8] Negm, A.M., Tarek, M.A., Mohamed, N.S., Wessam, Y. Impact of future discharges on Damietta branch morphology. In Fifteenth International Water Technology Conference, IWTC. Alexandria, Egypt, 2011.

[9] Ahmed, A.A, Fawzi, A. Meandering and bank erosion of the River Nile and its environmental impact on the area between Sohag and El-Minia, Egypt. Arabian Journal of Geosciences, 2011, 4, 1-11.

[10] Alesheikh, A.A., Ghorbanali, A., Nouri, N. Coastline change detection using remote sensing. International Journal of Environmental Science & Technology, 2007, 4, 61-66.

[11] Masria, A., Negm, A.M., Iskander, M. Assessment of Nile Delta coastal zone using remote sensing. The Nile Delta, 2016, In.: Springer.

[12] Mosselman, E. Theoretical investigation on discharge-induced river-bank erosion, Faculty of Engineering Delft University of Technology, 1989, 1-63.

[13] Li, X., Zhou, Y., Zhang, L. Kuang, R. Shoreline change of Chongming Dongtan and response to river sediment load: A remote sensing assessment. Journal of Hydrology, 2014, 511, 432-442.

[14] Canty, M.J., Image analysis, classification and change detection in remote sensing: With algorithms for ENVI/IDL and Python, Second edition, Taylor & Francis Group, 2014.

[15] Brice, J.C., Channel patterns and terraces of the Loup Rivers in Nebraska, US: Government Printing Office, 1964.